

CLEARING MAGNET DESIGN FOR APS-U*

M. Abliz†, J. Grimmer, Y. Jaski, F. Westferro and M. Ramanathan
Argonne National Laboratory, Argonne, IL 60439, U.S.A

Abstract

The Advanced Photon Source is in the process of developing an upgrade (APS-U) of the storage ring. The upgrade will be converting the current double bend achromat (DBA) lattice to a multi-bend achromat (MBA) lattice. In addition, the storage ring will be operated at 6 GeV and 200 mA with regular swap-out injection to keep the stored beam current constant [1].

The swap-out injection will take place with beamline shutters open. For radiation safety to ensure that no electrons can exit the storage ring, a passive method of protecting the beamline and containing the electrons inside the storage ring is proposed. A clearing magnet will be located in all beamline front ends inside the storage ring tunnel. This article will discuss the features and design of the clearing magnet scheme for APS-U.

INTRODUCTION

The APS-U will be operating the storage ring with regular swap-out injection as frequently as every 5 seconds. During these injections, the beamlines will be operating with the shutters open, and, as part of radiation safety, no electrons are allowed to exit the storage ring enclosure. Therefore, as part of the beamline, a passive device located inside the storage ring tunnel will be employed to ensure that the electrons cannot exit the storage ring enclosure.

A permanent magnet dipole (clearing magnet) will be located in the front end (part of the beamline between the storage ring exit and the concrete wall to the beamline) to deflect any electrons escaping the storage ring, to prevent them from exiting through the front end apertures and on to the experiment floor.

PRINCIPLE

The front end consists of various masks and shutters to collimate and stop the beam when needed. The main component which can fully contain the beam is the safety shutter, made of tungsten, located at about 22.7 m from the source point. Figure 1 is a schematic representation of the clearing magnet and associated relevant components in the high heat load front end (HHLFE). The clearing magnet is located immediately after a mask (FM2), and is 4 m upstream of the safety shutter. Based on the geometry of possible beam locations at the source, the worst case of mis-steered beam is shown in Fig. 1 below. The worst

case beam trajectory is when the electrons are 0.3 cm below the plane at the source and pass through the top of FM2, resulting in a beam offset of 0.63 cm above the nominal beam plane at the clearing magnet. Given the allowed overlap at the shutter, the required deflection here is 6.08 mrad. Taking the whole picture with the additional 0.44 mrad of the incident electron trajectory, the minimum total deflection to be produced by the clearing magnet is 6.52 mrad downwards. The APS-U storage ring is expected to be operated nominally at 6.0 GeV. However, as part of the safety envelop, the maximum energy of the electron for the magnet design has to be 10% more, resulting in assumptions of 6.6 GeV electrons to be deflected by 6.52 mrad for all calculations.

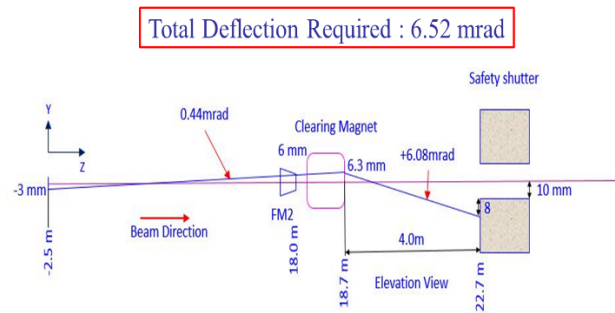


Figure 1: Schematic diagram of the clearing magnet location in the high heat load front end (HHLFE).

Based on these guiding principles the specifications for the clearing magnet are as shown in Table 1 below.

Table 1: Specifications for the Clearing Magnet

Parameter	Value	Unit
Ring Energy	6.6	GeV
Deflecting Angle	6.52	mrad
Gap	1.8	cm
Insertion Length	30	cm
Deflecting direction (electron beam)	Toward floor	---
Distance of the safety shutter from the clearing magnet	400	cm
Deflecting range in vertical (Y)	± 0.6	cm
Field at 20 cm from the magnet center	≤ 1	G

MAGNETIC DESIGN

A permanent magnet (PM) dipole was designed to produce a field of about 1T for a magnetic gap of 1.8 cm. An H-shaped hybrid PM dipole, that creates a B_x field, was designed with Opera 3D as shown in Fig. 2. The beam direction is along the Z-axis and the magnetic gap of 1.8 cm is along the X-axis. For this reference design, the magnet material of choice is NdFeB in grade N42SH, from Shin-Etsu Rare Earth Magnet, and the pole material is 1010 steel (soft iron). The N42SH has the following properties: $B_r = 1.27$ T (20°C) and intrinsic demagnetiza-

* Work supported by the U. S. Department of Energy, Office of Science, under Contract No. DE-AC02-06CH11357

† email address: mabliz@aps.anl.gov

tion field, $H_{cj} = 21$ kOe (20°C), thermal coefficient of $B_r = -0.11$ ($\% / ^\circ\text{C}$) and thermal coefficient of $H_{cj} = -0.52$ ($\% / ^\circ\text{C}$). The bh-curve for this design was set for a temperature of 25°C , which is the expected maximum temperature of the storage ring at the APS.

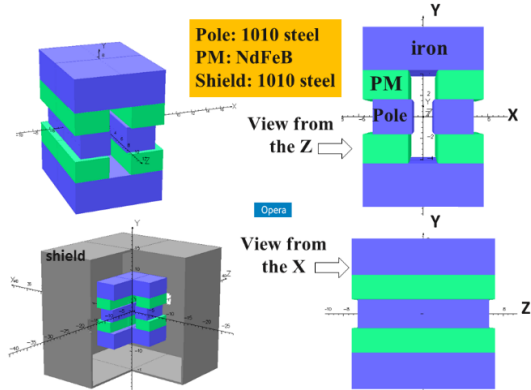


Figure 2: Different views of the clearing magnet. The blue colored parts are 1010 steel, the green colored parts are PMs, and the grey is 1010 steel for the shield.

The magnets are recessed 0.3 cm back from the pole tips as shown in the right top image in Fig. 2. The magnets are 1 cm longer than the poles as shown in the right bottom image. The thickness of the iron parts on the top and bottom is 3.74 cm. A 0.5 cm thick shield was placed 7.75 cm away from the magnet to contain all stray fields for safety. The dimensions of the magnets and poles are shown in Table 2. Figure 3 (a) shows a 2D magnetic flux distribution of the clearing magnet.

Table 2: Dimension of the PM and Poles

parameter	dimension	unit	parameter	dimension	unit
Magnet type	Hybrid dipole	—	PM recess	0.3	cm
Gap	1.8	cm	PM width	4	cm
Pole width	3.5	cm	PM height	2.5	cm
Pole height	3	cm	PM length	13.5	cm
Pole length	12.5	cm	PM chamfers	0.1	cm
Pole chamfers	0.1	cm			

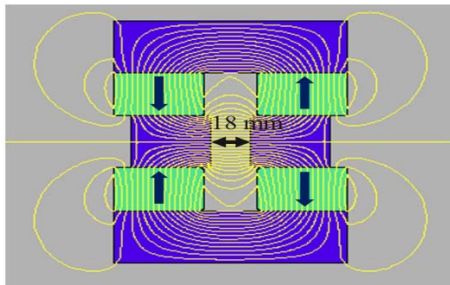


Figure 3: Magnetic flux distribution of the clearing magnet in a XY-plane. The green colored parts are PMs, and blue colored parts are 1010 steel;

Figure 4 shows the B_x field along the beam direction (Z) at 3 different Y positions as modeled with Opera 3D.

The field at Y of $+0.6$ cm is more important than the field at Y of -0.6 cm due to the deflection of the electron beam being towards the ground.

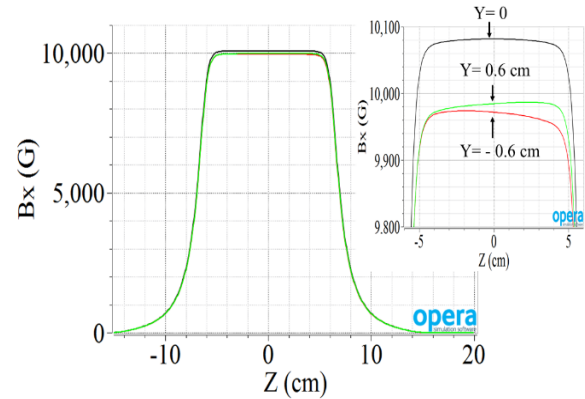


Figure 4: B_x field along the beam direction at 3 different Y positions. Z of 0 is the middle of the clearing magnet. The top inset plot is an enlargement over a smaller range of Z .

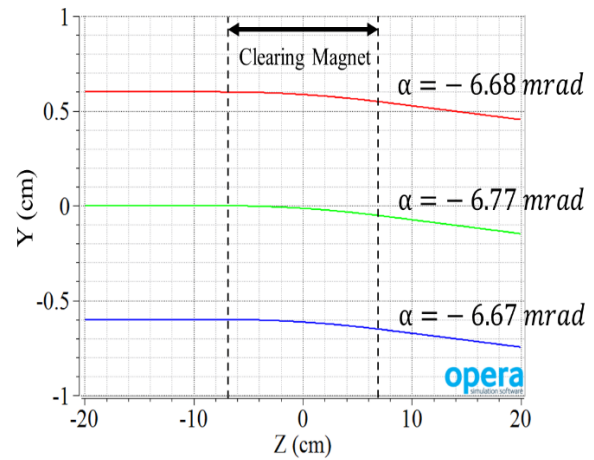


Figure 5: Electron beam trajectory through the clearing magnet with a ring energy of 6.6 GeV. The outgoing angle, α , was determined at the zero field region at the downstream end of the magnet.

Based on these fields, the trajectory for 6.6 GeV electrons was calculated. Figure 5 shows the trajectories of the 6.6 GeV electron beam at 3 different Y locations as it passes through the clearing magnet. The outgoing angle, α , was defined as the trajectory at the zero field region ($Z=20$ cm) at the downstream end of the clearing magnet. The outgoing angle of the electron beam is -6.77 mrad at the beam mid-plane ($Y = X = 0$). The differences in the outgoing angles of the beam, as shown in figure 5, are due to the small field differences, as shown in the inset of Fig. 4. As seen in Fig. 5, the worst case for Y at 0.6 cm is -6.68 mrad which is more than the required 6.52 mrad as shown in Table 1.

5: Beam Dynamics and EM Fields

D10 - Beam-Beam Effects - Theory, Simulations, Measurements, Code Developments

MECHANICAL DESIGN

The magnetic force on the YZ-plane at $X=0$ as simulated is shown in Fig. 6. The integrated force on the plane was 3814 N at an 1.8 cm gap (typical operational gap).

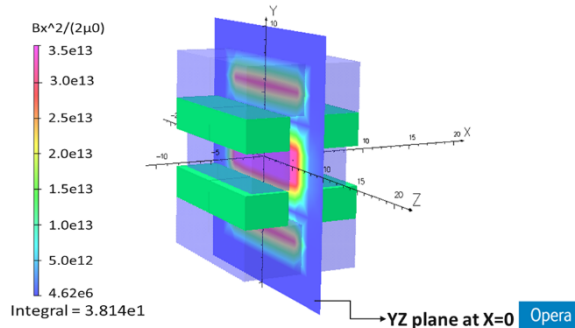


Figure 6: Magnetic force on a YZ-plane at $X=0$ at 1.8 cm gap. The color zone shows the force distribution at the plane. The iron parts are translucent.

Due to the large forces involved, the mechanical design has to take into consideration the assembly and maintenance processes. Towards this end, the magnet was split into two halves along the YZ plane. The splitting of the magnet has two-fold advantage: for ease of assembly, and also for operational purposes, when the vacuum chamber between the magnets has to be baked for vacuum conditioning. Hence the magnetic forces were calculated as a function of the gap between the two halves. Figure 7 is a plot of the force as a function of the magnetic gap. As expected, the force decreases exponentially with increasing gap.

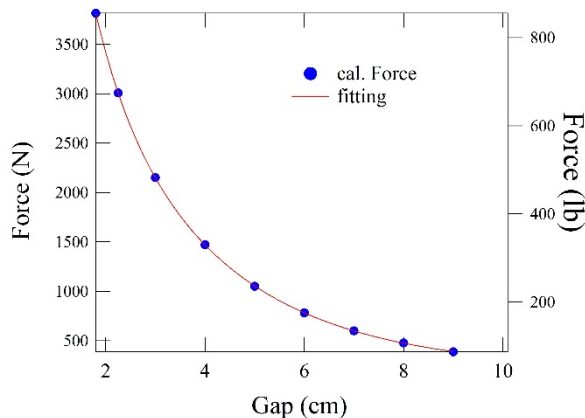


Figure 7: Magnetic force on the YZ-plane at $X=0$ at different gaps. The filled circles are the calculated forces from the model of the clearing magnet, and the red curve is the fitting.

Figure 8 is a conceptual model of the clearing magnet with the integrated vacuum chamber and all associated support systems. The top left model is in its operating condition. The top right is the end view of the clearing magnet when the two halves are separated for vacuum baking of the vacuum chamber in the middle. The bottom model is a rendering of the complete assembly with the two magnets shown separated. The mechanical design

takes into consideration the forces and has force compensation spring to assist in assembly and disassembly.

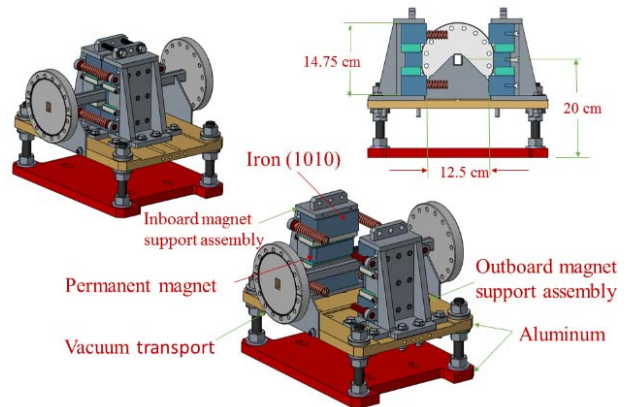


Figure 8: Three different views of the mechanical model of clearing magnet and its associated support systems.

DISCUSSION AND CONCLUSION

A clearing magnet based on hybrid permanent magnet assemblies was designed for the high heat load front end (HHLFE) of APS-U. The design was optimized to get the required B_x field integral efficiently [3]. This clearing magnet produces fields greater than 1T at a magnetic gap of 1.8 cm with fairly small permanent magnets.

In this design, the permanent magnets are recessed 0.3 cm back from the poles, thereby decreasing the B_x field at the center of the gap. However, this helps to decrease the maximum demagnetization field on the PM edges. The absolute maximum H_y field on the PM was 9.9 kOe for this design, which allows for the temperature to rise up to 80°C before demagnetization effects start affecting the magnet.

To minimize shunting of the magnetic field, the shields were placed as far from the magnet structure as reasonably possible, based on the space constraint within the front end. The shield keeps the stray fields fully contained as there are other storage ring magnets in close proximity, and also provides personnel safety.

The mechanical design takes into consideration the large forces and is designed to allow for ease of assembly and maintenance.

Overall, the design parameters for the clearing magnet for the high heat load front end were achieved, with a design that can be readily assembled, installed and maintained.

REFERENCES

- [1] R. Abela *et al.*, in *Proc. EPAC92*, 486-488, 1992.
- [2] Y. Jaski, F. Westferro, S. H. Lee, B. Yang, M. Abliz, and M. Ramanathan, "Conceptual Design of Front Ends for the Advanced Photon Source Multi-bend Achromats Upgrade" in *Proc. SRI 2015*, July 2015.
- [3] Y. Iwashita, T. Mihara, et al., "Permanent Magnet Quadrupole for Final Focus for Linear Collider" in *Proc. PAC2003*, May 2003.